

# Local defect in a magnet with long-range interactions

José A. Hoyos\* and Thomas Vojta†

*Department of Physics, University of Missouri-Rolla, Rolla, Missouri, 65409, USA.*

(Dated: November 18, 2021)

We investigate a single defect coupling to the square of the order parameter in a nearly critical magnet with long-range spatial interactions of the form  $r^{-(d+\sigma)}$ , focusing on magnetic droplets nucleated at the defect while the bulk system is in the paramagnetic phase. To determine the static droplet profile, we solve a Landau-Ginzburg-Wilson action in saddle point approximation. Because of the long-range interaction, the droplet develops a power-law tail which is energetically unfavorable. However, as long as  $\sigma > 0$ , the tail contribution to the droplet free energy is subleading in the limit of large droplets; and the free energy becomes identical to the case of short-range interactions. We also consider the effects of fluctuations and find that they do not change the functional form of the droplet as long as the bulk system is noncritical. Finally, we study the droplet quantum dynamics with and without dissipation; and we discuss the consequences of our results for defects in itinerant quantum ferromagnets.

PACS numbers: 75.10.Jm, 75.10.Nr, 75.40.-s

## I. INTRODUCTION

In a nearly critical system, a local defect that prefers the ordered phase can induce the nucleation of a droplet of local order in the nonordered background. Such droplets arise, e.g., in disordered systems due to the presence of rare strongly coupled spatial regions. They can have surprisingly strong consequences for the properties of the phase transition. In a classical magnet at nonzero temperature, a large finite-size droplet does not have a static magnetization; instead it fluctuates very slowly because flipping the droplet requires coherently changing the order parameter in a large volume. More than 30 years ago, Griffiths<sup>1</sup> showed that rare regions and the magnetic droplets formed on them, lead to a singularity in the free energy in a whole temperature region above the critical point, which is now known as the Griffiths region or the Griffiths phase.<sup>2</sup> Later, it was shown that this singularity is only an essential one<sup>3,4,5</sup> and thus probably unobservable in experiment (see also Ref. 6).

The effects of magnetic droplets are greatly enhanced if the underlying defects are extended macroscopic objects (linear or planar defects). In these cases, the droplet dynamics is even slower and so increases their effects. This was first found in the McCoy-Wu model,<sup>7,8</sup> a 2D Ising model with linear defects. Later it was studied in great detail in the context of the quantum phase transition of the random transverse-field Ising model where the defects are extended in the imaginary time dimension.<sup>9,10</sup> In these systems, the Griffiths singularity in the free energy actually takes a power-law form, and the susceptibility diverges inside the Griffiths region.

Recently, it has been shown that even stronger effects than these power-law Griffiths singularities can occur in Ising magnets with planar defects.<sup>11,12</sup> Droplets that are extended in two dimensions can undergo the magnetic phase transition (and develop a static order parameter) independently from the bulk system. This leads to a destruction of the global sharp phase transition by smear-

ing. (Note that an unusual magnetization-temperature relation was already found in the numerical mean-field analysis, Ref. 13, but it was interpreted as power-law critical behavior with a very large exponent  $\beta$ .) Similar smeared phase transitions have also been found in a non-equilibrium system in the presence of linear defects<sup>14</sup>. A recent review of these and other rare region effects can be found in Ref. 15.

One particularly interesting class of problems concerns droplets in metallic quantum magnets. In these systems, the dynamics of the magnetic modes is overdamped because they couple to gapless fermionic excitations. In metallic (Ising) antiferromagnets, this dissipative environment strongly suppresses tunneling, and sufficiently large droplets completely freeze at low temperatures.<sup>16,17,18</sup> The global quantum phase transition is thus smeared.<sup>19</sup>

In metallic ferromagnets, the situation is further complicated because the coupling between the magnetic modes and the gapless fermionic degrees of freedom generates an effective long-range spatial interaction between the magnetic fluctuations.<sup>20,21,22</sup> This interaction which takes the form  $r^{-(2d-1)}$  for clean electrons and  $r^{-(2d-2)}$  for diffusive electrons, where  $d \geq 2$  is the spatial dimensionality, can be viewed as a result of generic scale invariance (for a recent review see Ref. 23). Understanding defects in nearly critical metallic quantum ferromagnets thus leads to the question of whether the existence and the properties of magnetic droplets are influenced by the long-range spatial interaction.

In this paper, we therefore develop the theory of a single defect coupling to the square of the order parameter in a nearly critical classical or quantum magnet with power-law spatial interactions of the form  $r^{-(d+\sigma)}$  with  $\sigma > 0$  to ensure a proper thermodynamic limit. A crucial effect of the long-range interactions is that the tail of the magnetic droplet decays into the bulk region like a power-law of the distance as mandated by Griffiths theorem.<sup>24</sup> Such a strong tail extending into the region that prefers

the disordered phase can be expected to be energetically unfavorable. To find out to what extent this hinders the formation of the magnetic droplet, we study the droplet free energy within the saddle-point approach. In the quantum case, we also consider the tunneling dynamics of the droplet for three cases: undamped dynamics, overdamped dynamics due to Ohmic dissipation, and a conserved overdamped dynamics as in the itinerant ferromagnet.

Our paper is organized as follows: We introduce our model, a classical or quantum  $\phi^4$ -theory with long-range spatial interactions, in Sec. II. In Sec. III, we analyse the free energy of a droplet within saddle-point approximation, and we discuss fluctuations. The droplet dynamics in the quantum case is considered in Sec. IV. The concluding Sec. V is devoted to a summary as well as a discussion of the order parameter symmetry and the consequences of our results for quantum Griffiths effects.

## II. THE MODEL

In this section we introduce our model, a  $d$ -dimensional Landau-Ginzburg-Wilson field theory with long-range power-law interactions for a scalar order parameter field  $\varphi$ . We first formulate the model for the case of a zero-temperature quantum phase transition, and we later discuss the necessary changes for a classical thermal phase transition. The action of our quantum  $\phi^4$ -theory reads

$$S = S_{\text{stat}} + S_{\text{dyn}}, \quad (1)$$

with the static part given by

$$S_{\text{stat}} = \int d\tau \int dx dy \varphi(\mathbf{x}, \tau) \Gamma(\mathbf{x}, \mathbf{y}) \varphi(\mathbf{y}, \tau) + \frac{u}{2} \int d\tau dx \varphi^4(\mathbf{x}, \tau). \quad (2)$$

Here,  $\mathbf{x}$  and  $\mathbf{y}$  are position vectors and  $\tau$  is imaginary time. The bare two-point vertex,  $\Gamma(\mathbf{x}, \mathbf{y}) = \Gamma_{\text{NI}}(\mathbf{x})\delta(\mathbf{x} - \mathbf{y}) + \Gamma_{\text{I}}(\mathbf{x}, \mathbf{y})$ , contains a non-interacting part and the attractive long-range interaction. The latter is given by

$$\Gamma_{\text{I}}(\mathbf{x}, \mathbf{y}) = -\gamma \left[ \xi_0^2 + |\mathbf{x} - \mathbf{y}|^2 \right]^{-\left(\frac{d+\sigma}{2}\right)}. \quad (3)$$

Here,  $\gamma$  is the interaction strength,  $\xi_0$  is a microscopic cutoff length scale of the order of the lattice constant, and  $\sigma$  controls the range of the interaction. To ensure a proper thermodynamic limit (an extensive free energy),  $\sigma$  must be positive. Note that an additional short-range interaction of the usual form  $|\nabla\varphi|^2$  can be added, if desired. As will be shown in Sec. III A, its contribution is subleading. The noninteracting part of the vertex reads

$$\Gamma_{\text{NI}}(\mathbf{x}) = t_0 + \delta t(\mathbf{x}) + \Gamma_0, \quad (4)$$

where  $t_0$  is the bulk distance from criticality,<sup>42</sup> and the constant  $\Gamma_0$  is chosen such that it cancels the ( $\mathbf{q} = 0$ )

Fourier component of the interaction (thus ensuring that the bulk critical point is indeed at  $t_0 = 0$ ). It takes the value  $\Gamma_0 = \Omega_d \gamma \xi_0^{-\sigma} B(\sigma/2, d/2)/2$ . Here  $\Omega_d$  is the surface of a  $d$ -dimensional unit sphere, and  $B(x, y)$  is Euler's beta function.  $\delta t(\mathbf{x})$  is the defect potential. For definiteness we consider a single spherically symmetric defect at the origin,

$$\delta t(\mathbf{x}) = \begin{cases} -V & (|\mathbf{x}| < a) \\ 0 & (|\mathbf{x}| > a) \end{cases}. \quad (5)$$

We are interested in the case  $V > 0$ , i.e., in defects that favor the ordered phase.

When discussing the quantum tunneling dynamics of the magnetic droplets in Sec. IV, we will compare three different dynamical actions. (i) In the undamped case, the dynamical action is given by

$$S_{\text{dyn}}^{(1)} = T \sum_{\omega_n} \int d\mathbf{q} \frac{\omega_n^2}{c^2} |\tilde{\varphi}(\mathbf{q}, \omega_n)|^2 \quad (6)$$

where  $\tilde{\varphi}(\mathbf{q}, \omega_n)$  is the Fourier transform of the order parameter field in terms of wave number  $\mathbf{q}$  and Matsubara frequency  $\omega_n$ ,  $T$  is the temperature, and  $c$  plays the role of a velocity of the undamped modes.

(ii) If the magnetic modes are coupled to an ohmic bath, the leading term in the dynamic action takes the form

$$S_{\text{dyn}}^{(2)} = \tilde{\alpha} T \sum_{\omega_n} \int d\mathbf{q} |\omega_n| |\tilde{\varphi}(\mathbf{q}, \omega_n)|^2, \quad (7)$$

where  $\tilde{\alpha}$  measures the strength of the dissipation, and there is a microscopic frequency cutoff  $|\omega_n| < \omega_{\text{mic}}$ .

(iii) Finally, we also consider the case of overdamped dynamics with order parameter conservation analogous to the itinerant ferromagnet. The leading term in the dynamic action is given by

$$S_{\text{dyn}}^{(3)} = \tilde{\alpha}_c T \sum_{\omega_n} \int d\mathbf{q} \frac{|\omega_n|}{q} |\tilde{\varphi}(\mathbf{q}, \omega_n)|^2. \quad (8)$$

The action defined in Eqs. (1) to (8) describes a system close to a *quantum* phase transition. In order to investigate a droplet in a system close to a *classical thermal* phase transition, we simply drop the dynamical piece of the action and eliminate the imaginary time-dependence of the order parameter field.

## III. EXISTENCE OF MAGNETIC DROPLETS

In this section we investigate to what extent the existence of droplets is influenced by the long-range spatial interaction. The basic idea is as follows: If the local potential  $t_0 - V$  on the defect is negative, magnetic order is preferred on the defect even though the bulk system may be nonmagnetic,  $t_0 > 0$ . Figure 1 shows a schematic of

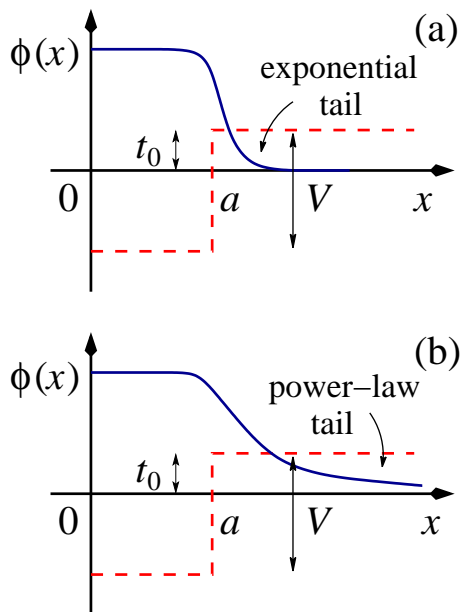


FIG. 1: (Color online) Schematic local order parameter profiles for defect induced droplets for short-range (a) and long-range (b) interactions. The dashed line depicts the defect potential.

the local order parameter profile in this situation, comparing short-range and long-range interactions. In the short-range case, the tail of the droplet profile falls off exponentially outside the defect.<sup>17,18,25</sup> Thus the tail provides only a subleading surface term to the droplet free energy. In contrast, for the long-range interaction (3), the tail must take a power-law form because Griffiths theorem<sup>24</sup> dictates that the magnetic correlations cannot decay faster than the interaction. The tail thus extends far into the bulk region where the local potential is positive, and therefore leads to a large positive contribution to the droplet free energy. In this section we study whether this mechanism hinders the formation of magnetic droplets for long-range interactions.

### A. Saddle-point equation

We start by analyzing the action (1) within saddle-point approximation, focusing on the case  $t_0 > 0$  (non-critical bulk system) because it is relevant for Griffiths phenomena. We can restrict ourselves to time-independent solutions because they have the lowest saddle-point actions (any time dependence produces an extra, strictly positive contribution from  $S_{\text{dyn}}$ ). Setting  $\varphi(\mathbf{x}, \tau) = \phi(\mathbf{x})$  and minimizing the total action with respect to this field leads to the saddle-point equation

$$(t_0 + \delta t(\mathbf{x}) + \Gamma_0) \phi(\mathbf{x}) + u\phi^3(\mathbf{x}) = \int \frac{\gamma \phi(\mathbf{y}) d\mathbf{y}}{[\xi_0^2 + |\mathbf{x} - \mathbf{y}|^2]^{\frac{d+\sigma}{2}}}. \quad (9)$$

Note that the classical action discussed at the end of section II leads to the same saddle-point equation. Therefore, the remainder of this section applies to both the classical and quantum cases.

We have not managed to solve the nonlinear integral equation (9) in closed form. We therefore first present analytical results for the behavior of  $\phi(\mathbf{x})$  far away from the defect, and then we complement them by a numerical solution. For sufficiently large  $V$  (such that  $t_0 - V$  is sufficiently negative), we expect the order parameter in the droplet core,  $|\mathbf{x}| < a$ , to be roughly constant. Griffiths' theorem<sup>24</sup> mandates that the droplet tail cannot decay faster than  $|\mathbf{x}|^{-(d+\sigma)}$ ; we therefore try the spherically symmetric ansatz

$$\phi(\mathbf{x}) = \begin{cases} \phi_0 & (|\mathbf{x}| < a) \\ C/|\mathbf{x}|^{d+\sigma} & (|\mathbf{x}| > a) \end{cases}, \quad (10)$$

with parameters  $\phi_0$  and  $C$ . Note that in general, the ansatz (10) is not continuous at  $|\mathbf{x}| = a$ . To cure this unphysical behavior, there must be an intermediate region  $a < |\mathbf{x}| < a + \xi_m$  which connects the core with the asymptotic region in (10). We will come back to this point later in this section.

We now insert the ansatz (10) into the saddle-point equation (9) and analyze it in the limit of large defects,  $a \gg \xi_0$ , and large distance,  $|\mathbf{x}| \gg a$  where (9) can be linearized in  $\phi$ . We find that the ansatz indeed solves the linearized saddle-point equation with the amplitude  $C$  given by (to leading order in  $a$ )

$$C = \frac{\Omega_d \phi_0 \gamma}{dt_0} a^d. \quad (11)$$

Note that  $C$  diverges when the bulk system approaches criticality ( $t_0 \rightarrow 0$ ) indicating that the ansatz (10) is not valid for a defect in a *critical* bulk. We will come back to this point in the next subsection.

To determine  $\phi_0$ , we now calculate the saddle-point action by inserting the solution (10) with (11) into the action (1). The result is the sum of a droplet core term, a tail term, and a core-tail interaction term. The core term takes the form  $(\Omega_d/d)a^d \phi_0^2 (t_0 - V + u\phi_0^2/2)$ . The contribution of the long-range interaction is exactly cancelled by the  $\Gamma_0$ -term, as must be the case for a constant order parameter. Interestingly, the tail term and the core-tail interaction term are subleading in the limit of large defects,  $a \gg \xi_0$ . Their leading  $a$ -dependencies are  $a^{d-2\sigma}$  and  $a^{d-\sigma-1}$  (up to possible logarithmic corrections), respectively. Finally, we have to consider the intermediate region  $a < |\mathbf{x}| < a + \xi_m$  in which droplet core smoothly connects to the asymptotic tail. From the numerical solution of the saddle-point equation (discussed in the next subsection) we found that the width of the intermediate region is of the order of the microscopic scale,  $\xi_m \sim \xi_0$  (at least as long as the bulk system is not too close to criticality; see next subsection for details). Importantly,  $\xi_m$  does not depend on the defect size  $a$ . Therefore, the intermediate region can at most make a surface-type con-

tribution to the droplet free energy, i.e., it can at most scale like  $a^{d-1}$ .

Collecting all the terms, we find that the saddle-point action takes the form

$$S_{\text{SP}} = \frac{\Omega_d}{d} \phi_0^2 a^d \left( t_0 - V + \frac{u}{2} \phi_0^2 \right) + \mathcal{O}(a^{d-1}, a^{d-2\sigma}) \quad (12)$$

in the limit of a large defect ( $a \rightarrow \infty$ ). Minimizing  $S_{\text{SP}}$  with respect to  $\phi_0$  gives the optimal value

$$\phi_0 = \sqrt{\frac{V - t_0}{u}}. \quad (13)$$

This means, in the limit of a large defect, a droplet of local order starts to form as soon as the local potential  $t_0 - V$  on the defect becomes negative. For finite  $a$ , the subleading terms in (12) lead to a shift in the onset of local order that can be described by finite-size scaling in the usual way.

The results (12) and (13) are identical to the case of short-range interactions.<sup>17,18,25</sup> We thus arrive at the somewhat surprising conclusion that even though the long-range interactions do induce a power-law tail of the droplet, they do not change the leading behavior of its free energy (in the limit of large defects), and thus do not hinder the existence of large droplets.

We also note that an additional short-range interaction of the form  $|\nabla\phi|^2$  in the static action (2) will not modify our results. Clearly, in the core region of the droplet it plays no role, and faraway from the core ( $\mathbf{x} \gg a$ ), it only produces a subleading power-law. Its contribution in the intermediate region can at most be of order  $a^{d-1}$ .

## B. Fluctuations

So far, we have analyzed the magnetic droplets within saddle-point approximation. In this subsection we discuss to what extent fluctuations modify the above saddle-point analysis. It is useful to divide the fluctuations into two classes, small fluctuations about the saddle-point solution and collective reorientations of the entire droplet in (imaginary) time. These two classes are well separated if the local order on the defect is properly developed, i.e.,  $V - t_0 \gtrsim u$ . The collective reorientations determine the long-time quantum dynamics of the droplet. They will be considered in more detail in Sec. IV.

In contrast, small long-wavelength fluctuations could potentially modify the droplet profile (10), in particular the form of the magnetization tail. To study the relevance of these fluctuations, we expand the action (1) about the saddle-point solution and perform a tree-level (power-counting) renormalization group analysis. The results depend qualitatively on whether or not the bulk system is critical.

As long as the bulk system is in its disordered phase,  $t_0 > 0$ , the asymptotic long-distance decay of the droplet magnetization is controlled by the *stable* large- $t_0$  fixed

point of the bulk rather than its critical fixed point. Since this stable fixed point does not have anomalous dimensions, the saddle-point analysis is qualitatively correct and the decay exponent in (10) remains unchanged. Thus, the fluctuations only renormalize nonuniversal prefactors. Analogous results were found in Ref. 17 for the case of short-range case interaction. Note that critical fluctuations *on the defect* can change the exponent in the relation (13) close to the onset of local order at  $t_0 - V = 0$ , provided the system is below its upper critical dimension. However, this has no bearing on the form of the tail.

In contrast, if the bulk system is right at the transition,  $t_0 = 0$ , the long-distance magnetization decay is controlled by the exponent  $\eta$  of the *critical* fixed point via  $\phi(\mathbf{x}) \sim |\mathbf{x}|^{-d+2-\eta}$  (because far from the defect,  $\phi(\mathbf{x})$  falls off as the bulk correlation function). For a classical magnet with long-range interactions this fixed point was studied in the seminal work of Fisher, Ma, and Nickel.<sup>26</sup> They found that the critical behavior is mean-field-like for  $\sigma < d/2$  with  $\eta = 2 - \sigma$ . For  $\sigma > 2 - \eta_{\text{SR}}$  (where  $\eta_{\text{SR}}$  is the exponent of the corresponding short-range model), the critical behavior is identical to that of the short-range model.<sup>27,28,29</sup> In between, the exponents are nonclassical and interpolate between mean-field and short-range behavior. Lets us also point out that interesting crossover phenomena occur when the bulk system is close but not exactly at the critical point. In this case the critical fixed point controls the magnetization decay at intermediate distances (of the order of the bulk correlation length) from the defect while the asymptotic behavior is again given by the saddle-point result (10).

## C. Numerical solutions of the saddle-point equation

In this subsection we confirm and complement the asymptotic analysis of the saddle-point equation (9) by a numerically exact solution.

We study both one and three space dimensions. In the three-dimensional case, for a spherical defect and droplet, the angular integration on the r.h.s. of the saddle-point equation (9) can be carried out analytically leading to a one-dimensional integral equation in radial direction. We now discretize space in units of the microscopic length  $\xi_0$  and fix the energy scale by setting  $u = 1$ . The resulting set of nonlinear equations is solved by the following procedure: We start from an ansatz for  $\phi$  (e.g., the ansatz given in (10)) and numerically perform the integral in the long-range term of (9). We then determine an improved value for  $\phi$  by solving the remaining cubic equation at each point by standard methods. These steps are repeated iteratively until the solution converges.

In this way, we have analyzed one-dimensional systems with  $2 \times 10^4$  to  $2 \times 10^5$  points and three-dimensional systems with  $10^4$  to  $10^5$  points in radial direction. We have studied the cases  $\sigma = 1, 2, 3$ , large defects  $a \gg 1$

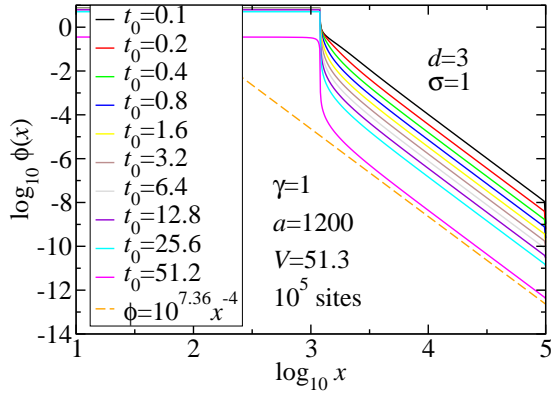


FIG. 2: (Color online) Local order parameter  $\phi$  of a three-dimensional droplet as a function of distance  $x$  from the defect center for different distances  $t_0 = 0.1$  to  $51.2$  from bulk criticality.

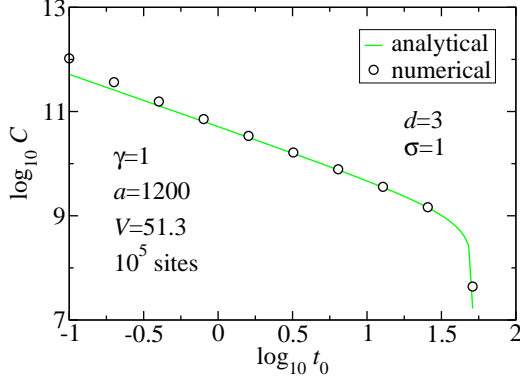


FIG. 3: (Color online) Amplitude  $C$  of the asymptotic power-law decay of the droplet tail for the system shown in Fig. 2. The solid line is the theoretical prediction, Eqs. (11) and (13).

and various values of  $t_0$ ,  $V$  and  $\gamma$ . For weak long-range interactions and away from bulk criticality, our procedure converges rapidly. With increasing  $\gamma$  and decreasing  $t_0$ , the convergence becomes slower. However, in all cases, our self-consistency cycle eventually converges, giving us a numerically exact solution of the saddle-point equation.

We now present and discuss a few characteristic results from these calculations. In Fig. 2, we show saddle-point solutions for  $d = 3$ ,  $\sigma = 1$  and different values of the distance  $t_0$  from bulk criticality. In agreement with the analytical predictions of the last subsection, the order parameter is essentially constant on the defect. For large  $|\mathbf{x}|$ , the droplet tail falls off with the predicted power-law  $\phi \sim |\mathbf{x}|^{-(d+\sigma)} = |\mathbf{x}|^{-4}$  for all values of  $t_0$ . The amplitude  $C$  of this power-law decay is analyzed in Fig. 3. As predicted in the last subsection, for small  $t_0$ ,  $C$  behaves like  $1/t_0$  (the small deviations are the lowest  $t_0$  stem from the fact that in these cases,  $10^5$  sites is not sufficient to reach the asymptotic regime).

Figure 4 shows the dependence of the droplet profile

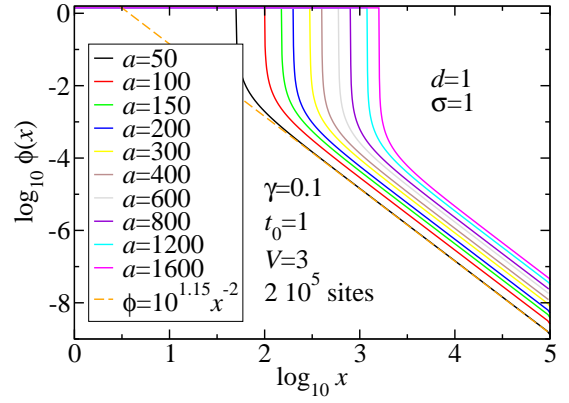


FIG. 4: (Color online) Local order parameter  $\phi$  of a one-dimensional droplet as a function of distance  $x$  from the defect center for different defect sizes  $a = 50$  to  $1600$  (from left to right).

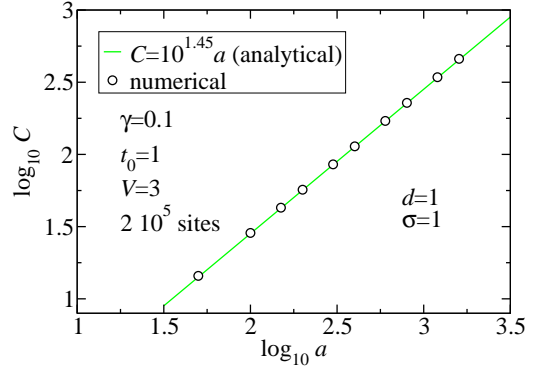


FIG. 5: (Color online) Amplitude  $C$  of the asymptotic power-law decay of the droplet tail for the system shown in Fig. 4. The solid line is the theoretical prediction, Eqs. (11) and (13).

on the size  $a$  of the defect for a system with  $d = \sigma = 1$ . For all  $a$ , the asymptotic decay of the droplet tail takes the predicted power-law form,  $\phi \sim |\mathbf{x}|^{-(d+\sigma)} = |\mathbf{x}|^{-2}$ . This figure also shows that the width  $\xi_m$  of the intermediate  $\mathbf{x}$ -region which connects the droplet core with the power-law tail does not change with  $a$  as discussed in the last subsection. (This becomes even more obvious when a linear rather than the logarithmic  $x$ -scale is used.) Moreover, in agreement with (13),  $\phi_0$  does not depend on  $a$ . The amplitude  $C$  of this power-law decay is analyzed in Fig. 5. In agreement with the theoretical prediction (11), the amplitude grows linearly with the defect size  $a$ .

We have performed analogous calculations for other parameter sets, including varying  $t_0$  for  $a = 300, 600, 1600$  as well as varying  $a$  for  $V = 30$ . In all cases, we have found excellent agreement with the predictions of the asymptotic analysis of Sec. III C.

#### IV. TUNNELING DYNAMICS

In this section, we study the tunneling dynamics of a single droplet at a zero-temperature quantum phase transition. Our approach starts from the pioneering work of Callan and Coleman<sup>30</sup> and Leggett and coworkers<sup>31,32</sup> (in the case of dissipative dynamics). In the following subsections we separately discuss the droplet dynamics for the three dynamical actions given in Eqs. (6) to (8), starting with the undamped case.

##### A. Undamped magnet

Following Callan and Coleman<sup>30</sup>, the tunneling rate between the *up* and *down* states of the droplet (i.e., the tunnel splitting of the ground state) can be estimated from the action of instanton-like saddle-point solutions  $\varphi(\mathbf{x}, \tau)$  fulfilling the boundary conditions  $\varphi(\mathbf{x}, \tau) \rightarrow \pm\phi(\mathbf{x})$  for  $\tau \rightarrow \pm\infty$ . In principle, several processes contribute to the overall tunneling rate. In the simplest one, the droplet retains its shape while collapsing and reforming.<sup>33,34</sup> A competing process consists of the nucleation of a domain wall that then sweeps the droplet.<sup>35</sup>

We start by considering the collapse-and-reformation process which can be described by an ansatz

$$\varphi(\mathbf{x}, \tau) = \phi(\mathbf{x}) \eta(\tau) \quad (14)$$

with  $\phi(\mathbf{x})$  being the static saddle-point solution of section III and  $\eta(\tau) \rightarrow \pm 1$  for  $\tau \rightarrow \pm\infty$ . Inserting this ansatz into the action (1) and integrating over the spatial variables yields the following excess effective action (above the time-independent solution  $\eta \equiv 1$ )

$$\Delta S^{(1)} = \frac{\Omega_d}{d} \phi_0^2 a^d \int d\tau \left[ \frac{\phi_0^2 u}{2} (1 - \eta^2)^2 + \frac{1}{c^2} \left( \frac{d\eta}{d\tau} \right)^2 \right] \quad (15)$$

to leading order in the defect size  $a$ . The saddle-point instanton solution of this action can be found exactly. It takes the form  $\eta(\tau) = \tanh(\tau/\tau_0)$ , with  $\tau_0^{-2} = c^2 \phi_0^2 u/2$ . The resulting instanton action reads

$$\Delta S_{\text{inst}}^{(1)} = \frac{4\Omega_d}{3d} u \phi_0^4 a^d \tau_0 \quad (16)$$

giving a tunnel splitting

$$\omega^{(1)} \approx \omega_0 e^{-\Delta S_{\text{inst}}^{(1)}}. \quad (17)$$

The ‘‘attempt frequency’’  $\omega_0$  can be determined by standard quantum tunneling considerations<sup>32</sup> from the fluctuations about the instanton solution. Importantly, the tunneling rate decays exponentially with the volume of the droplet. Equations (15) to (17) are in complete agreement with the corresponding results for the case of short-range interactions,<sup>17,18,36</sup> reflecting the fact that the leading terms of the instanton action stem from the droplet core rather than the tail.

To discuss the contribution of the moving domain wall processes to the tunneling rate, we use the ansatz

$$\varphi(\mathbf{x}, \tau) = \phi(\mathbf{x}) \eta(\tau - x/v) \quad (18)$$

which describes a domain wall that sweeps the droplet in  $x$ -direction with velocity  $v$ .  $\eta$  describes the domain wall shape and fulfills the boundary conditions  $\eta(z) \rightarrow \pm 1$  for  $z \rightarrow \pm\infty$  as before. Inserting this into the action (1) gives the same effective action (15) plus one additional positive term from the spatial dependence of  $\eta$  (this term corresponds to the domain wall energy). Therefore, the minimal action for this process is bounded by (16), and to exponential accuracy the corresponding tunnelling rate cannot be larger than (17). This is in qualitative agreement with earlier results for short-range interactions. Stauffer<sup>35</sup> estimated the tunneling rate of a domain wall within quasiclassical WKB approximation and found that it depends exponentially on the droplet volume. Senthil and Sachdev<sup>37</sup> estimated the tunnel splitting of a locally ordered island in a transverse-field Ising model using perturbation arguments. Again, the result (which should contain all possible processes) is exponentially small in the droplet volume.

##### B. Overdamped dynamics

We now consider overdamped dynamics with the action  $S_{\text{dyn}}^{(2)}$  as given in (7). Inserting the ansatz  $\varphi(\mathbf{x}, \tau) = \phi(\mathbf{x}) \eta(\tau)$  into  $S_{\text{dyn}}^{(2)}$  and integrating over the spatial variables gives the following contribution to the effective action

$$\Delta S^{(2)} = \frac{\Omega_d}{d} a^d \phi_0^2 \int d\tau d\tau' \frac{\tilde{\alpha}}{2\pi} \frac{(\eta(\tau) - \eta(\tau'))^2}{(\tau - \tau')^2} \quad (19)$$

to leading order in the defect size  $a$ . The other terms are as in eq. (15). A straight forward saddle-point instanton analysis of the effective action analogous to the last subsection fails because the interaction of the trajectory  $\eta(\tau)$  at large positive times with the trajectory at large negative times causes a logarithmic divergence. Following Refs. 32 and 38, the calculation therefore proceeds in two stages.

In the first stage, we introduce a *low-frequency* cutoff  $\omega_c$  in the dynamic action (7). This changes the interaction kernel in (19),

$$\frac{1}{(\tau - \tau')^2} \rightarrow \frac{1 + 2\omega_c |\tau - \tau'|}{(\tau - \tau')^2 (1 + \omega_c |\tau - \tau'|)^2}, \quad (20)$$

and removes the divergence. We have not been able to solve analytically for the instanton but we have used the ansatz  $\eta(\tau) = \tanh(\tau/\tau_0)$  with variational parameter  $\tau_0$ . Minimizing the effective action  $\Delta S^{(1)} + \Delta S^{(2)}$  with respect to  $\tau_0$  gives

$$\tau_0 = \frac{3\tilde{\alpha}}{\pi \phi_0^2 u} \left( 1 + \sqrt{1 + \frac{2\pi^2 \phi_0^2 u}{9c^2 \tilde{\alpha}^2}} \right). \quad (21)$$

In the limit of weak dissipation,  $\tilde{\alpha} \rightarrow 0$ , we recover the result for undamped dynamics while strong dissipation,  $\tilde{\alpha} \rightarrow \infty$ , leads to  $\tau_0 = 6\tilde{\alpha}/(\pi\phi_0^2 u)$ . The resulting instanton action can be expressed in terms of the dimensionless dissipation strength parameter<sup>32,38</sup>

$$\alpha = \frac{4\Omega_d}{\pi d} \phi_0^2 a^d \tilde{\alpha}. \quad (22)$$

We note that  $\alpha$  is proportional to the defect volume  $a^d$ . (Analogous results have been obtained for dissipative random quantum Ising models.<sup>39,40</sup>) The dissipative part of the instanton action reads

$$\Delta S_{\text{inst}}^{(2)} = -\alpha \ln(\omega_c) + f(\alpha), \quad (23)$$

where the function  $f(\alpha)$  is given by  $f(\alpha) = c\alpha + O(\alpha^2)$  for weak dissipation and  $f(\alpha) = -\alpha \ln \alpha + c'\alpha + O(\ln(\alpha))$  for strong dissipation.  $c$  and  $c'$  are constants of order one. For comparison we have also studied a piecewise linear ansatz for  $\eta(\tau)$ . The resulting instanton action is identical to (23) except for different numerical values of the constants  $c, c'$ . At the end of the first stage of the calculation we thus obtain the bare tunnel splitting

$$\omega_{\text{bare}}^{(2)} \approx \omega_0 e^{-\Delta S_{\text{inst}}^{(2)}}. \quad (24)$$

In the second stage of the calculation the resulting dissipative two-level system is treated using renormalization group methods.<sup>32</sup> It is well-known that instanton-instanton interactions renormalize the tunnel splitting, yielding

$$\omega^{(2)} \sim \omega_{\text{bare}}^{(2)} \left[ \frac{\omega_{\text{bare}}^{(2)}}{\omega_c} \right]^{\alpha/(1-\alpha)}. \quad (25)$$

This also eliminates the unphysical dependence of the tunnel splitting on the arbitrary cutoff parameter  $\omega_c$ . We thus find that the smaller defects with  $\alpha < 1$  continue to tunnel, albeit with a strongly reduced rate. The larger defects with  $\alpha > 1$  cease to tunnel, i.e., they are on the localized side of the Kosterlitz-Thouless phase transition of the dissipative two-level system. These results are in qualitative agreement with the case of short-range interactions.<sup>17,18</sup>

### C. Conserved overdamped dynamics

Finally, we consider the case of overdamped dynamics with a conserved order parameter as given by the dynamic action (8). Such an action arises, e.g., in the case of an itinerant quantum ferromagnet.

Order parameter conservation requires some care in discussing the dynamics of our locally ordered droplet. In particular, the homogeneous magnetization  $\int d\mathbf{x} \varphi(\mathbf{x}, \tau)$  must not be time dependent. Therefore, the product form  $\varphi(\mathbf{x}, \tau) = \phi(\mathbf{x}) \eta(\tau)$  with  $\phi(\mathbf{x})$  the static solution of section III is not a suitable ansatz in this case. This

can be fixed (in a crude way) by subtracting a constant from the droplet profile,  $\phi'(\mathbf{x}) = \phi(\mathbf{x}) - \text{const}$  such that the  $\mathbf{q} = 0$  Fourier component is cancelled. The ansatz  $\varphi(\mathbf{x}, \tau) = \phi'(\mathbf{x}) \eta(\tau)$  then provides a variational upper bound for the instanton action.

Inserting this ansatz into (8) and carrying out the integral over the spatial variables leads to a dissipative term in the effective  $\eta(\tau)$  action with the same functional form as (19). The prefactor and the resulting dimensionless dissipation strength  $\alpha$ , however, are different. To leading order in the defect size  $a$ , we find

$$\alpha = \begin{cases} 8\phi_0^2 a^4 \tilde{\alpha}_c / \pi & (d=3) \\ 32\phi_0^2 a^3 \tilde{\alpha}_c / (3\pi) & (d=2) \end{cases}. \quad (26)$$

In general dimension  $d \geq 2$ , the dimensionless dissipation strength is now proportional to  $a^{d+1}$  instead  $a^d$ . The extra factor  $a$  compared to the non-conserved case in Sec. IV B can be understood as follows. To invert the magnetization of a droplet of linear size  $a$ , magnetization must be transported over a distance that is at least of order  $a$  (because the order parameter conservation prevents simply flipping the sign of the magnetization on the defect). This involves modes with wave vectors of the order of  $q \sim 1/a$ . Since the dissipation strength in (8) is inversely proportional to  $q$ , we expect an additional factor  $a$  in the effective action. This argument strongly suggests that this extra factor is *not* an artefact of our simple ansatz for  $\varphi(\mathbf{x}, \tau)$  but correctly reflects the physics of the conserved order parameter case.

In all other respects, the calculation proceeds as in the non-conserved case in Sec. IV B. The resulting dynamic behavior of the droplets depends on the value of the dimensionless dissipation strength parameter  $\alpha$ . Small droplets ( $\alpha < 1$ ) still tunnel while the larger ones ( $\alpha > 1$ ) freeze. Because  $\alpha$  is now proportional to  $a^{d+1}$  the tunneling of large droplets is even more strongly suppressed than in the non-conserved case.

## V. DISCUSSION AND CONCLUSIONS

To summarize, we have studied the physics of a single defect coupling to the square of the order parameter in a nearly critical system with long-range spatial interactions of the form  $r^{-(d+\sigma)}$  with  $\sigma > 0$ . Such a defect can induce the nucleation of a magnetic droplet while the bulk system is still in the nonmagnetic phase. Due to the long-range interactions, the droplet magnetization develops a long power-law tail, i.e., at large distances  $r$  from the defect, it decays like  $r^{-(d+\sigma)}$  in agreement with Griffiths' theorem.<sup>24</sup> Nonetheless, the droplet free energy is dominated by the core (on-defect) contribution while the tail contribution is subleading in the limit of large defects. Therefore, droplets will nucleate on large defects as soon as the local potential (the local distance from criticality) becomes negative, in complete agreement with the case of short-range interactions. Our explicit calculations of the droplet magnetization profile have been performed

within saddle-point approximation, but as long as the bulk system is noncritical, fluctuations do not change the functional form of the droplet. They only renormalize nonuniversal parameters.

In addition to the existence of the magnetic droplets, we have also investigated their dynamics. As is well known,<sup>15</sup> in the case of a classical (thermal) phase transition, the droplet cannot order statically. Instead, it fluctuates between ‘up’ and ‘down’ due to thermal fluctuations. For a zero-temperature quantum phase transition, the behavior is potentially different, depending on the form of the dynamic action. We have studied three cases. In the absence of dissipation, even very large droplets can always tunnel, but with a rate that decreases exponentially with the droplet volume. This changes in the presence of (Ohmic) dissipation. The qualitative behavior now depends on the dimensionless dissipation strength  $\alpha$ . For  $\alpha < 1$ , the droplet still tunnels albeit with a further reduced rate while for  $\alpha > 1$ , tunneling ceases and the droplet magnetization becomes static. For overdamped dynamics without order parameter conservation,  $\alpha$  is proportional to the volume of the droplet core. Thus, sufficiently large droplets always freeze in agreement with Refs. 16,17,18. In the case of overdamped dynamics with order parameter conservation as in the itinerant quantum ferromagnet, the dissipation effects are further enhanced because the dimensionless dissipation strength  $\alpha$  for a droplet of linear core size  $a$  is proportional to  $a^{d+1}$  rather than  $a^d$ .

Let us comment on the order parameter symmetry. Our explicit results have been for the case of a scalar (Ising) order parameter. However, the analysis of the droplet existence in Sec. III relied on saddle-point arguments and thus applies equally to continuous  $O(N)$  order parameters with  $N > 1$ . In contrast, to generalize the discussion of the dynamics in Sec. IV to such order parameters, other types of fluctuations (rotational ones)

must be considered.

We also emphasize that we have discussed the case of an isotropic attractive long-range interaction. Droplet *formation* dominated by oscillating and/or anisotropic interactions such as the dipolar or the RKKY interactions is likely of different type and not considered here.

Finally, we briefly discuss the consequences of our results for the (quantum) Griffiths effects in systems with long-range spatial interactions. Because the power-law magnetization tail only makes a subleading contribution to the free energy of a magnetic droplet, such droplets can form on rare (strongly coupled) spatial regions of the disordered system essentially in the same way as in the case of short-range interactions. Therefore, as long as droplet-droplet coupling can be neglected, the Griffiths effects should be identical to those in short-range interacting systems. However, it is clear that the droplet-droplet coupling is more important for long-range interactions than for short-range ones. This means, it must be considered for lower droplet density and, in the quantum case, for higher temperatures. The complicated physics caused by the coupling of several droplets is beyond the scope of this paper. Recently, it has been argued<sup>41</sup> that this coupling can qualitatively change the Griffiths effects at least in some cases. A complete understanding of this phenomenon remains a task for the future.

## Acknowledgments

We gratefully acknowledge discussions with J. Schmalian and M. Vojta. This work has been supported by the NSF under grant no. DMR-0339147, and by Research Corporation. We also thank the Aspen Center for Physics, where part of this work has been performed.

\* Electronic address: hoyosj@umr.edu

† Electronic address: vojtat@umr.edu

<sup>1</sup> R. B. Griffiths, Phys. Rev. Lett. **23**, 17 (1969).

<sup>2</sup> M. Randeria, J. P. Sethna, and R. G. Palmer, Phys. Rev. Lett. **54**, 1321 (1985).

<sup>3</sup> M. Wortis, Phys. Rev. B **10**, 4665 (1974).

<sup>4</sup> A. B. Harris, Phys. Rev. B **12**, 203 (1975).

<sup>5</sup> A. J. Bray and D. Huifang, Phys. Rev. B **40**, 6980 (1989).

<sup>6</sup> Y. Imry, Phys. Rev. B **15**, 4448 (1977).

<sup>7</sup> B. M. McCoy and T. T. Wu, Phys. Rev. Lett. **21**, 549 (1968).

<sup>8</sup> B. M. McCoy and T. T. Wu, Phys. Rev. **176**, 631 (1968).

<sup>9</sup> D. S. Fisher, Phys. Rev. Lett. **69**, 534 (1992).

<sup>10</sup> D. S. Fisher, Phys. Rev. B **51**, 6411 (1995).

<sup>11</sup> T. Vojta, J. Phys. A **36**, 10921 (2003).

<sup>12</sup> R. Sknepnek and T. Vojta, Phys. Rev. B **69**, 174410 (2004).

<sup>13</sup> B. Berche, P. E. Berche, F. Igloi, and G. Palagyi, J. Phys. A **31**, 5193 (1998).

<sup>14</sup> T. Vojta, Phys. Rev. E **70**, 026108 (2004).

<sup>15</sup> T. Vojta, J. Phys. A **39**, R143 (2006).

<sup>16</sup> A. H. Castro Neto and B. A. Jones, Phys. Rev. B **62**, 14975 (2000).

<sup>17</sup> A. J. Millis, D. K. Morr, and J. Schmalian, Phys. Rev. Lett. **87**, 167202 (2001).

<sup>18</sup> A. J. Millis, D. K. Morr, and J. Schmalian, Phys. Rev. B **66**, 174433 (2002).

<sup>19</sup> T. Vojta, Phys. Rev. Lett. **90**, 107202 (2003).

<sup>20</sup> T. Vojta, D. Belitz, R. Narayanan, and T. R. Kirkpatrick, Europhys. Lett. **36**, 191 (1996).

<sup>21</sup> T. Vojta, D. Belitz, R. Narayanan, and T. R. Kirkpatrick, Z. Phys. B **103**, 451 (1997).

<sup>22</sup> D. Belitz, T. R. Kirkpatrick, and T. Vojta, Phys. Rev. B **55**, 9452 (1997).

<sup>23</sup> D. Belitz, T. R. Kirkpatrick, and T. Vojta, Rev. Mod. Phys. **77**, 579 (2005).

<sup>24</sup> R. B. Griffiths, J. Math. Phys. **8**, 478 (1967).

<sup>25</sup> R. Narayanan, T. Vojta, D. Belitz, and T. R. Kirkpatrick,



- Phys. Rev. B **60**, 10150 (1999).
- <sup>26</sup> M. E. Fisher, S.-K. Ma, and B. G. Nickel, Phys. Rev. Lett. **29**, 917 (1972).
- <sup>27</sup> J. Sak, Phys. Rev. B **8**, 281 (1973).
- <sup>28</sup> E. Luijten and H. W. J. Blöte, Phys. Rev. Lett **89**, 025703 (2002).
- <sup>29</sup> J. Cardy, *Scaling and renormalization in statistical physics* (Cambridge University Press, Cambridge, 1996).
- <sup>30</sup> C. G. Callan and S. Coleman, Phys. Rev. D **16**, 1762 (1977).
- <sup>31</sup> A. O. Caldeira and A. J. Leggett, Ann. Phys. (N.Y.) **149**, 374 (1983).
- <sup>32</sup> A. J. Leggett, S. Chakravarty, A. T. Dorsey, M. P. A. Fisher, A. Garg, and W. Zwerger, Rev. Mod. Phys. **59**, 1 (1987).
- <sup>33</sup> C. P. Bean and J. D. Livingston, J. Appl. Phys. **30**, S120 (1959).
- <sup>34</sup> E. M. Chudnovsky and L. Gunther, Phys. Rev. Lett. **60**, 661 (1988).
- <sup>35</sup> D. Stauffer, Sol. State. Commun. **18**, 533 (1976).
- <sup>36</sup> J. A. Hoyos and T. Vojta, unpublished.
- <sup>37</sup> T. Senthil and S. Sachdev, Phys. Rev. Lett. **77**, 5292 (1996).
- <sup>38</sup> A. T. Dorsey, M. P. A. Fisher, and M. S. Wartak, Phys. Rev. A **33**, 1117 (1986).
- <sup>39</sup> G. Schehr and H. Rieger, Phys. Rev. Lett. **96**, 227201 (2006).
- <sup>40</sup> J. A. Hoyos and T. Vojta, Phys. Rev. B **74**, 140401 (2006).
- <sup>41</sup> V. Dobrosavljevic and E. Miranda, Phys. Rev. Lett. **94**, 187203 (2005).
- <sup>42</sup> In principle, one must distinguish between the bare and the renormalized distance from the critical point. We will suppress this difference unless otherwise noted, because it is of no importance for our considerations.